(4)

Technical Document 1799
April 1990

Gain, Pulse Power Distribution, and Single Electron Counting Efficiency of P-20, P-47, and X-3 Phosphors

University of Arizona

TABLE OF CONTENTS

ABSTRACT

Analysis has been made of the dc gain, the pulse power distribution (PPD) and the single photoelectron counting efficiency of P-20, P-47 and X-3 phosphors. The results have been obtained by testing fully operating image intensifiers as well as by examining phosphor screen samples using a scanning electron microscope. Two P-47 intensifiers were manufactured by ITT with the screens processed in identically the same way as the screens used in the diode front end of the NOSC hybrid detector. A new two-dimensional photon counter has been constructed to detect single photoelectron pulses and to measure the PPD of even the NOSC poorly-focused proximity diode intensifier, as well as other intensifiers.

The dc gain in Proxitronic P-20 intensifiers has been improved to a consistently very high figure (greater than 450 photons/15-kV-photoelectron) through optimizing the phosphor layer thickness and the electron scrubbing dosage. Similar optimizing has been carried out in Proxitronic X-3 phosphors, resulting in a gain figure of about 110 photons/15-kV-photoelectron. The gains of the two ITT P-47 tubes were measured to be 92 and 115 photons/15-kV-photoelectron, respectively. Sandwich gains with an appropriately matched photocathode fiberoptically coupled to these phosphors are characteristically around 60 for the P-20, 12 for the X-3 and 15 for the P-47. Higher figures could be expected for glass-out/glass-in coupling, such as used in the non-imaging NOSC hybrid detector.

The present optimized Proxitronic tubes exhibit as high a counting efficiency (60%) as any other P-20 (and P-11 and Z-151B) phosphor tubes we have examined in 15 years, with the exception of an occasional Varo tube that was made with a magic potion P-20. We have been unable to duplicate in a P-20 phosphor the high counting efficiency (85%) exhibited by at least some Varo P-20 intensifier diodes manufactured in the late 70s and early 80s, nor have we determined why these phosphor screens were so good. Early Proxitronic P-20 intensifiers were found to have insufficient phosphor screen thickness, resulting in about a 10% area of voids and a comensurate loss in gain and counting efficiency. However, of all the other screen production processes we have examined as candidates for causing lost counting efficiency, none was found to have an effect.

The two ITT P-47 phosphor tubes and two Proxitronic X-3 phosphor tubes all exhibit virtually ideal 100% counting efficiencies when operated at 15 kV. This is in spite of the fact that neither phosphor has as high an energy efficiency as the P-20 in converting electrons to light.

At operating voltages of 10 kV and higher, all three phosphor types (P-20, P-47 and X-3) produce a double-peaked PPD. The present two-dimensional photon counter is free enough of

low-power noise to clearly discern the presence of the second low-power peak. The majority of pulses in the low-power peak represent a multiple-counting of the original photoelectron, and are thought to possibly be caused by X-rays. This multiple counting gives rise to integrated raw counting efficiency values of greater than 100% at sufficiently low pulse powers. However, the statistical fluctuations in the pulses demonstrate that the statistical counting efficiency, or true counting efficiency, is substantially lower than the integrated raw counting efficiency at 0 power.

In tests of the P-47 phosphor tubes, as the voltage is lowered below about 10 kV, the separation between the main peak and the low-power peak of the PPD becomes more and more obscure, the main peak melding with the low-power peak. For pulse counting, this makes it increasingly difficult to discriminate between a true photoelectron pulse and a false multiple-counting event or other noise pulse at low powers. For analog detectors, such as the NOSC detector, the broadened PPD will degrade the noise factor of the system. At a voltage of 6 kV, the PPD is very skew toward low power, and some of the photoelectrons appear to become truly lost (73 % statistical counting efficiency).

We conclude that the lost photoelectron pulses in most P-20 screens (and P-11 and Z-151B screens that have exhibited low counting efficiencies of about 50% as well) is caused by a flaw that occurs during the initial manufacture of the phosphor powder. Our current hypothesis is that there exists insufficient activator density, and thereby insufficient target areas, in the presently manufactured powders. The high counting efficiency P-47 and X-3 phosphors are fabricated with activator densities typically 3 to 5 times that of P-20 powders. There is some evidence that a high energy electron trapping mechanism may exist in the low counting efficiency phosphors that removes some electrons from hitting a target at all.

Recommeded future work includes carrying out a more detailed examination of the noise processes taking place in the low-power region of the P-47 PPD, determining the operating voltage at which photoelectron pulses are definitely lost in the P-47, constructing a P-20 phosphor with higher activator density, examining a high-activator-density thulium-activated phosphor, and measuring the S/ performance under field conditions of the NOSC hybrid detector as a function of diode high voltage.

I. INTRODUCTION

This report summarizes research carried out at Steward Observatory that was sponsored in part under the NOSC Contract N66001-86-C-0311, Detector Evaluation and Phosphors Development. The total time period over which this research was conducted was from 9/1/86 to 12/30/88.

Prior to this investigation, we had discovered that many of the image intensifier systems used as primary detectors in astronomical instruments fail to record nearly half of the photoelectrons released from their photocathodes. The reason for this is that many first stage photoelectrons released in an image intensifier simply fail to produce any measurable light pulse whatsoever when they strike the first phosphor screen. This "lost photon" problem is characteristic of image intensifiers produced by many different manufacturers, and is a problem of several commonly used types of phosphor screens. Our understanding of the low electron counting efficiency of phosphor screens up to the beginning of our new work has been published (Cromwell, 1986). We are pleased to report that during the present program we have come to further understand, and have considerably improved, the single photoelectron counting efficiency of phosphors used in image intensifiers.

Early in the new work, several tube samples having P-20 phosphor screens were manufactured by Proxitronic. The tubes were made with varying phosphor screen deposition techniques in the hopes of determining the specific cause-and-effect of low counting efficiency. With the interesting, but disappointing results that followed, we decided to take an entirely new approach to studying the problem. Besides just directly measuring the photoelectron counting efficiency in operating image intensifiers, we used a scanning electron microscope to observe for the very first time the extremely fine-scale cathodoluminescent properties of individual phosphor grains. These tests ultimately led to our realization that no step undertaken by Proxitronic in the screen production process was responsible for damaging the phosphor, at least when such processes were kept within common, reasonable bounds. Rather, it seems most likely that one or more steps employed by the manufacturer of the phoshpor powder proper (Riedel de Haen in West Germany) is at fault. Our present hypothesis is that there exists an insufficiently high number-density of activity centers in a phosphor grain (determined in part by the proportion of activator used in fabricating the phosphor) so that a single high-energy photoelectron often entirely fails to excite the grain to emit light. Support for this idea has come from our recent tests of tubes comprised of phosphor screens other than P-20. In these tubes, with P-47 and X-3 phosphors, phosphors that utilize a higher proportion of activator than is used in the earlier P-20 phosphors, counting efficiencies near the ideal 100 % are measured.

In the sections that follow, more detailed discussions are given of the major tests carried out during this program.

II. TWO-DIMENSIONAL PHOTON COUNTER

An important goal in the present study was to employ for the NOSC ITT proximity intensifier the same accurate analysis methods we had developed in the past to analyse many intensified photon counters (Cromwell et. al. 1985, Allen et. al. 1984, Hege et. al. 1979). Our past system was designed to analyse image data in only one dimension (ie spectroscopic, or line-imaged, data). The NOSC ITT proximity intensifier does not produce sharply enough focused images to permit analysis with our past system. We therefore developed a full two-dimensional photon counting system that could image the entire output of the NOSC intensifier, or any other intensifier. Then, by treating the NOSC intensifier as an imaging detector, most of our previous analysis methods could be employed virtually in tact, with little modification. To accomplish this, we replaced our Reticon dual linear array readout device with a Pulnix CCD standard television camera, shown in Fig 1. The CCD camera images are read into a video frame grabber installed in a PC. Development of the software employed with the frame grabber to create a two-dimensional photon counting system and a pulse-power analysing system was a major effort in the present program. The result is a system which greatly improves the speed (by at least a factor 20) and accuracy with which we can assess the photcelectron pulse power distribution and counting efficiency of image tubes.

We modified the high-quality, well-documented 4-stage Varo intensifier package (Steward Observatory's "Big Red" detector) to provide a means of highly amplifying sample single-stage tubes. The fiberoptic output screen of the intensifier under test is directly fiberoptically coupled to the input photocathode of Big Red, as illustrated in Fig. 1. The phosphor output of Big Red is continuously read out by the CCD television camera. Provided a single photoelectron from the sample tube causes a bright enough scintillation on its output phosphor that two or more secondary electrons are emitted by Big Red's input photocathode, each photoelectron event from the sample intensifier will be clearly detected as a bright pulse of light by the CCD camera. Because the probability of detection is 85% for single electrons emitted by Big Red's photocathode, the probability of detecting a phosphor scintillation from a coupled sample tube releasing two or more secondaries is virtually 100%. The primary characteristics of the two-dimensional photon counter may best be illustrated in the following description of the method for determining the pulse power distribution and photoelectron counting efficiency of a sample image intensifier.

III. MEASUREMENT OF PULSE POWER DISTRIBUTION AND PHOTOELECTRON COUNTING EFFICIENCY

The photocurrent in the sample intensifier is measured with an electrometer while a uniform circular image of light is projected onto its photocathode. The projected image is then attenuated a calibrated amount and the projector shutter is repeatedly opened for 10 ms once every 5 seconds. (Emphasis is placed on the careful calibration of the attenuation of the light source, as the attenuation factor can otherwise be a large source of error in such an experiment). The central wavelength and passband of the light source are defined by an interference filter in the projector (4250 A, 200 A fwhm). A blue central wavelength is selected so as to avoid changes in photocathode response as a function of high voltage of the proximity focused intensifier. Typically, about 100 photoelectrons are released from the sample tube photocathode during each triggering of the shutter. The source shutter is synced to the CCD video readout, so that all photoelectrons are released during the first 10 ms of a 33 ms integration time of the 30 frames-a-second standard television readout system. The frame grabber captures and stores four consecutive 1/30-second TV fields; the first two fields are "dark fields", where no light was incident on the sample tube's front photocathode, the third field is the "flash field", where the source shutter was triggered, and the fourth field is another "dark field", although the image is comprised mostly of phosphor afterglow images of the photoelectron pulses released during the previous "flash field". To avoid the effects of the phosphor afterglow images (in either dark or flash fields), and to prevent counting phosphor afterglow images as bonafide new pulses, the computer subtracts, pixel by pixel, the respective previous field from the flash field and from the dark field to be analysed. The subtraction is done over a roughly square picture area of 7x7 mm comprised of 170 horizontal by 200 vertical pixels (covering substantially more area than the roughly 6 mm diameter circular image). The result is two subtracted pictures, one a flash picture and the other a previous-field dark picture, each of which contain images of only new pulses that occured during their respecive integration time, and each devoid of any phosphor afterglow images.

A pulse finding program then locates all pulse image peaks in the flash and dark pictures, identifies any "blended" pulses (where only one pixel separates two adjacent pulse peaks), and then computes the power of each bonafide unblended pulse by summing its signal over a 3 by 3 pixel grid centered about each peak. The pulse power measured in this way is expressed in terms of single digital A/D units from the frame grabber. Typically, a pulse intensity profile measures less than 2 pixels fwhm, and the f/stop of the relay lens is adjusted so that the very brightest pixels do not exceed the 8 bit limit per pixel of the framegrabber (ie, 255). Code in the pulse finding program

tests for pulses that are saturated at 255, and assures that pulses that are comprised of two or more adjacent saturated pixels remain properly "flat-topped" after subtraction of a previous field. The program also identifies ion events by virtue of their high power and breadth. The pulse finding and power measuring process is repeated for each new pair of flash and dark pictures until roughly 100 picture pairs have been measured (and therefore roughly 10,000 photoelectron pulses have been accumulated from the flash pictures). Histograms are created of the number of pulses counted vs. their power. Corrections are applied for the few number of blended pulses. The dark histogram is subtracted from the flash histogram. The resulting number of pulses counted is divided by the known number of original photoelectrons released, and a final histogram is generated that gives the observed pulse power distribution (PPD), expressed as a probability of detection of the known number of photoelectrons.

The PPD of the two-dimensional photon counting system Big Red alone is shown in Fig. 2. All pulses counted that are brighter than 1000 A/D units are summed and plotted in the highest power bin (labled >1000). The probability value for this last bin is divided by 10 so that it may be plotted on the same scale as the remaining histogram even in test situations where a large portion of the pulses are brighter than 1000. An integrated "raw counting efficiency" is computed by summing the PPD from the highest pulse power value to specific lower pulse power values. The raw counting efficiency is entered at various pulse powers along a row labled "R" in Fig. 2. Also entered is an integrated "statistical counting efficiency", labled "S", computed by squaring the ratio of the raw counting efficiency divided by its standard deviation. The PPDs plotted in Fig. 2 and other figures are histograms of the raw counts counted above dark emission during a test. The standard deviation of the statistical counting efficiency mean value is given in those instances where more than one 100-picture run was analysed. Typically the shape of the PPD is double peaked, and is comprised of a gaussian, or Poissonian, broad peak at some intermediate pulse power plus a second peak toward the very low pulse power end.

The peak at low power could in principle be caused by noise in the measuring instrument. However, this noise is commonly kept low by setting the peak-finding threshold to a value comfortably above the noise peaks of the instrument. Thus, the low-power peak in the PPD is, indeed, created mostly by the phosphor screen of the first stage intensifier. (That is, the phosphor screen of the first stage in Big Red in the case of Fig. 2, and the phosphor screen of the tube under test in the case of other PPDs shown in other figures). We have noted the presence of such a low-power peak in our earlier work (cf. Cromwell et al, 1985), but have previously simply extrapolated the main, Poissonian, portion of the curve toward zero pulse power to estimate the number of pulses in this "noisey" low-power region of the PPD. With the new two-dimensional photon

III. MEASUREMENT OF PULSE POWER DISTRIBUTION AND PHOTOELECTRON COUNTING EFFICIENCY

The photocurrent in the sample intensifier is measured with an electrometer while a uniform circular image of light is projected onto its photocathode. The projected image is then attenuated a calibrated amount and the projector shutter is repeatedly opened for 10 ms once every 5 seconds. (Emphasis is placed on the careful calibration of the attenuation of the light source, as the attenuation factor can otherwise be a large source of error in such an experiment). The central wavelength and passband of the light source are defined by an interference filter in the projector (4250 A, 200 A fwhm). A blue central wavelength is selected so as to avoid changes in photocathode response as a function of high voltage of the proximity focused intensifier. Typically, about 100 photoelectrons are released from the sample tube photocathode during each triggering of the shutter. The source shutter is synced to the CCD video readout, so that all photoelectrons are released during the first 10 ms of a 33 ms integration time of the 30 frames-a-second standard television readout system. The frame grabber captures and stores four consecutive 1/30-second TV fields; the first two fields are "dark fields", where no light was incident on the sample tube's front photocathode, the third field is the "flash field", where the source shutter was triggered, and the fourth field is another "dark field", although the image is comprised mostly of phosphor afterglow images of the photoelectron pulses released during the previous "flash field". To avoid the effects of the phosphor afterglow images (in either dark or flash fields), and to prevent counting phosphor afterglow images as bonafide new pulses, the computer subtracts, pixel by pixel, the respective previous field from the flash field and from the dark field to be analysed. The subtraction is done over a roughly square picture area of 7x7 mm comprised of 170 horizontal by 200 vertical pixels (covering substantially more area than the roughly 6 mm diameter circular image). The result is two subtracted pictures, one a flash picture and the other a previous-field dark picture, each of which contain images of only new pulses that occured during their respecive integration time, and each devoid of any phosphor afterglow images.

A pulse finding program then locates all pulse image peaks in the flash and dark pictures, identifies any "blended" pulses (where only one pixel separates two adjacent pulse peaks), and then computes the power of each bonafide unblended pulse by summing its signal over a 3 by 3 pixel grid centered about each peak. The pulse power measured in this way is expressed in terms of single digital A/D units from the frame grabber. Typically, a pulse intensity profile measures less than 2 pixels fwhm, and the f/stop of the relay lens is adjusted so that the very brightest pixels do not exceed the 8 bit limit per pixel of the framegrabber (ie, 255). Code in the pulse finding program

A/D units), there is considerable noise, and therefore uncertainty, in the statistical counting efficiency values. Therefore, for PPDs where an inadequate number of measurements was made, the statistical counting values are not entered for the low-power points.

IV. P-20 PHOSPHORS

Twelve sample tubes were manufactured by Proxitronic and were tested by Steward Observatory. Seven were "gain-stage" tubes, having fiberoptic input and output windows to facilitate fiberoptic coupling between stages, and five were first-stage configurations, having quartz input windows (for good uv transmission) and fiberoptic output windows. The gain-stage tubes were the first such Proxitronic tubes ever examined by Steward Observatory. The phosphor screens in most of the twelve samples were processed with slightly different screen thickness, grain diameter, bakeout temperature, and/or amount of electron scrubbing to continue our study into the parameters affecting phosphor gain and counting efficiency. The phosphor of one tube was produced by a "brush" technique (similar to that used by Varo) instead of the "settled-in-liquid" technique normally employed by Proxitronic. Measurements were made of the counting efficiency of the first stage tubes using our previous Reticon dual array photon counter. Measurements were also made of one of these tubes with the new two-dimensional photon counter. DC gain measurements were also made of the tubes.

Proxitronic also produced twelve samples of P-20 phosphor screens mounted on fiberoptic substrates for study using a scanning electron microscope (SEM). Each sample was made with a variation in the standard processing steps to study the influence of various steps on the cathodoluminescent properties of the phosphor grains. Samples included a screen where all normal steps were carried out, one containing a settled phosphor only (with no further steps), ones with differing thicknesses of lacquer films baked out (and one not baked out) at differing temperatures, ones with varying thicknesses of aluminum layers, one without the black aluminum layer, and ones with varying amounts of electron scrubbing. Considerable insight into the low counting efficiency problem has been gained through this new study, as listed below. A final report summarizing the SEM work was submitted to NOSC in April, 1987 (contract N66001-85-0203).

1. We find that the optimum thickness for both counting efficiency and dc gain is 1.1mg/sq.cm, roughly 1.5 times the thickness normally applied by Proxitronic. Thinner screens have areas of voids, where no phosphor particles exist, thus impairing dc gain and especially counting efficiency. Thicker screens only result in lower dc gain, as light that is emitted from the layer closest to the impinging electron side of the

screen is absorbed by grains that lie intermediate between the emitting grain and the output window. Figure 3 shows the dc gains vs. voltage of several P-20 phosphor tubes we have measured. The dc gains are expressed as the equivalent number of photons emitted by the phosphor near the peak of the phosphor's spectral output (5600 A for P-20) per incident photoelectron.

2. Modest electron scrubbing (0.4 microamp/sq.cm. for 1 hr) of the screen at elevated temperature preserves the inherent high dc gain of the phosphor grains while also safely removing possible contaminants. Higher scrubbing dosages, specifically those with higher current densities, result in lost dc gain. However, a high scrubbing dosage seems to not affect the counting efficiency of the screen.

3. The dc gain in recent optimized phosphor screens is consistently high (better than 450 photons/15 kV electron) and is more than a factor 2 better than early Proxitronic screens. These recent gain figures are the best we have measured in any P-20 screen from any other manufacturer (curve A in Fig. 3).

4. We have failed to produce another intensifier that duplicates the same high counting efficiency (70%) measured in one set of Proxitronic samples produced in 1985 (Cromwell et al, 1986), although the present optimized tubes are better on the average than earlier tubes. We have subsequently found that the high figure in this unique set of samples was a temporary phenomenon, and the long-term, stable value is similar to that of present tubes (about 60%). Figure 5a shows the PPD and counting efficiency of a recent Proxitronic P-20 tube. In this test with the two-dimensional photon counter, the relay lens f/stop was opened up so that a detailed look could be made at the low-power end of the PPD. The figure illustrates how the raw counting efficiency can substantially exceed 100%, yet the statistical counting efficiency plateaus to a value of roughly 56%. The latter value agrees well with the counting efficiency value determined using our older method and the photon counting Reticon system.

5. Regarding counting efficiency, our SEM and live tube studies have now shown that only one of the suspected problems, improper screen thickness, indeed causes low counting efficiency, and this is now well understood and has been corrected. However, none of the remaining plausible candidates that we have examined and that we had originally suspected might cause phosphor destruction appear to cause low counting efficiency. (The candidate causes we have investigated are listed in the first two paragraphs of this section).

6. The counting efficiency results above and especially the results of our SEM tests have led us to suspect that the cause of low counting efficiency in the Proxitronic P-20 phosphor tubes is an inadequate number of activity centers, or emission sites, within a phosphor grain. That is, an adequate

"target area" is not provided for an impinging single electron. (This we suspect is equally true in other manufacturers' tubes we have measured as well, including some with other types of phosphors). Thus, the problem can hopefully be solved in P-20 phosphors by modifying the method of original manufacture of the phosphor grains. As we shall see below, in the case of the P-47 and X-3 phoshors, the problem is already solved.

Because we had discovered several years ago that at least some Varo intensifiers having P-20 phosphor screens exhibited high counting efficiency (one example is Big Red discussed earlier), we attempted to find in our collection of rejected Varo tubes a sample with high counting efficiency so that we could dismantle it and examine the screen with the SEM. Unfortunately, the candidate tube turned out to have a poor counting efficiency (about 63%), so no further tests were made. The unique high counting efficiency of at least some Varo tubes manufactured in the late 70's and early 80's has remained an inspiration that we can develop again a P-20 phosphor having good counting efficiency. To our knowledge, the batch of magic potion P-20 powder once made for Varo has never since been duplicated, nor understood.

V. P-47 PHOSPHORS IN ITT TUBES

Two sample diode intensifiers were made by ITT having P-47 phosphor screens that were deposited using the same raw materials and techniques as are used for the proximity focused front-end intensifier of the NOSC ITT hybrid detector. However, the sample screens were deposited on fiberoptic faceplates rather than glass faceplates (the latter are used in NOSC tubes) in order to image and transfer the most light via fiberoptic coupling to our two-dimensional photon counter. The first tube was an electrostatically focused configuration and the second tube was proximity focused. The diameter of the electrostatically focused tube was 40 mm in order to provide at least a 10 mm diameter area having uniform resolution, geometry, and gain. The diameter of the proximity focused tube was 25 mm, and this tube provided good uniformity throughout its active field. The reason for making one sample an electrostatically focused tube was to minimize the confusing effects of scattered light and backscattered electrons (forming signal-induced background) that we had measured in earlier ITT proximity focused tubes (Cromwell et al, 1985). The proximity tube was made with increased spacing between its photocathode and phosphor compared to the NOSC tubes in order to allow operation up to 15 kV applied voltage.

Figure 4 shows the dc gain vs. voltage for the two P-47 phosphor intensifiers. The nearly identical slopes of the two curves illustrate that both screens have the same intrinsic

gain. The only significant difference between the two is in their "dead voltage" values, 2.8 kV for the electrostatic tube and 4.0 kV for the proximity tube. Presumably this difference is due to a different thickness of aluminum coating in the two screens, although ITT attempted to provide identical coatings to both.

As is the case for the P-20 screens shown in Fig. 3, the gain in Fig. 4 is expressed as the number of equivalent photons emitted by the phosphor per incident photoelectron, where the wavelength of the emitted photon is near the peak wavelength of the phosphor's spectral emission. Thus, for the P-47 phosphors in Fig.4 the photons are at a wavelength of 4250 A, whereas for the P-20 and X-3 phosphors in Fig. 3, the wavelength is 5600 A. With the gains expressed in this way, a quick and fairly accurate calculation may be made of the secondary electron gain (often called the "sandwich gain") of a photocathode coupled to the output of the phosphor by simply multiplying the gain times the coupling transfer efficiency (1.0 for a numerical aperture 1.0 input fiberoptic) times the quantum efficiency of the photocathode at the wavelength specified for the phosphor. (Sandwich gain is a dimensionless quantity that specifies the number of secondary electrons emitted per primary electron). For example, the quantum efficiency of Big Red's photocathode at 4250 A is 7.2 percent and at 5600 A is 11.4 percent. The input window to Big Red is a numerical aperture 1.0 fiberoptic faceplate. Thus, the secondary electron gain, or sandwich gain, at the coupling between the electrostatic P-47 tube shown in Fig. 4 and Big Red is 115x1x.072=8.3 when the electrostatic tube is at 15 kV, and is 30x1x.072=2.2 when the electrostatic tube is at 6 kV. (The sandwich gain in a NOSC hybrid tube may be estimated to have roughly 6 times higher sandwich gain, having a factor of 3 due to the higher transmission of the glass/glass coupling vs. the present fiberoptic/fiberoptic coupling, and a factor of 2 due to a photocathode optimized for the P-47 blue output). As another example, only this time for a P-20 phosphor, the sandwich gain at the coupling between the Proxitronic tube A in Fig. 3 and Big Red is 560x1x.114=63.8 when tube A is at 15 kV.

The PPDs and counting efficiencies of the two P-47 intensifiers are shown in Figs. 5, 6 and 7. In Fig. 5b, a detailed look at the low-power end of the PPD of the electrostatic P-47 tube is shown by opening up the relay lens, just as was done for the Proxitronic P-20 tube in Fig. 5a. In Figs. 6a through 6d are shown the results of the electrostatic P-47 tube at four different applied voltages: 15, 12, 8 and 6 kV. Figure 7 illustrates the PPD and counting efficiency of the proximity P-47 tube. Unlike any of the other tubes studied here, two curves are required to adequately represent the pulses emitted from the proximity P-47 tube. Fig. 7a shows the PPD of the pulses emitted within the normal 7x7 mm image area (the area that contains virtually 100% of the output pulses in all the other tubes), and Fig. 7b shows the PPD of pulses that are widely distributed throughout the remainder of the entire 25 mm

diameter field, pulses that occur outside the normal, centered, 7x7 mm analysis area. These pulses arise primarily from scattered light that was transmitted by the original photocathode and that was subsequently reflected back to the photocathode via the shiny aluminum layer of the phosphor screen. Such photoelectron pulses occur at a point well separated from the original image.

The important results from these measurements may be summarized as follows:

1) The statistical counting efficiency in both P-47 tubes reaches the virtually ideal 100%, even for operating voltages as low as 8 kV.

2) There exists a low-power second peak in the PPD of the P-47 phosphors similar to that seen in the P-20 phosphors. As discussed earlier in Section III, the low-power peak appears to be due to a multiple-counting phenomenon (eg., X-ray emission), such that the raw counting efficiency reaches an inflated value greater than 100% at low powers, while the statistical counting efficiency plateaus to a constant value that is the true counting efficiency (cf. Figs. 5b and 6a).

3) As the voltage is lowered below about 10 kV, the division between the main peak and the low-power peak of the PPD becomes more and more obscure, and the main peak effectively "broadens out" (ie, its fwhm becomes a larger percentage of its mean value). The main peak thus melds with, and becomes part of, the low-power peak. This progression is illustrated in Figs. 6a through 6d. For pulse counting, this makes it increasingly difficult at the lower operating voltages to discriminate between a true photoelectron pulse and a false multiple-counting event or other noise pulse at low powers. For analog detectors, such as the NOSC detector, the broadened PPD will of course degrade the noise factor of the system.

4) At a voltage of 6 kV, the PPD has become very skew toward low power, and some of the photoelectrons appear to become truly lost (73 % statistical counting efficiency at 6 kV vs. virtuallly 100 % at 8 kV). However, a more thorough examination than we have done here would need to be carried out of the statistical count at the extreme low-power end in order to say with certainty what happens to the very low-power pulses.

5) The proximity P-47 tube behaves similarly to the electrostatic P-47 tube, except that with the proximity tube one must include the pulses that occur considerably outside the primary image area due to scattered light. That is, the final PPD and counting efficiency for this tube is the sum of the respective values given in Fig. 7a plus those in Fig 7b. (If this proximity tube were to be used as an imaging detector, the scattered light would severely compromise its performance. However, when used merely as a non-imaging photoelectron amplifier in the NOSC application, such scattered light presents

no problem). The PPD of the area outside the image (shown in Fig. 7b) is comprised of relatively more low-power pulses than that of the primary image area (Fig. 7a). We suspect that this is because the fainter pulses in this outer area are comprised of relatively more pulses due to X-Rays and possibly also due to backscattered electrons that originally formed the primary image. (Note that the electrostatic tube will not generate pulses from backscattered electrons off its phosphor screen because of the zero electic field in the phosphor anode region of the electrostatic lens). Figure 7c shows the PPD of single electrons from Big Red alone, taken under identical test conditions to those of the proximity tube in Figs. 7a and 7b. Under these conditions, only the brightest third of the full Big Red alone PPD is captured. Figures 7a, b and c illustrate that the majority of even the lower power pulses from the P-47 phosphor release more than one Big Red electron. The reason that a prominent low-power peak is missing in the proximity tube PPDs in Figs. 7a and 7b, but is present in the electrostatic tube PPDs in Figs. 5b and 6a (15 kV operating voltage in all cases), is not due to any significant real difference between the PPDs of the two tubes. Rather, the apparent difference in the figures is due simply to different test conditions: the pulses of the proximity tube were of relatively lower brightness when they were imaged onto the photon counter CCD, due to the respective tube gains and the relay lens settings used.

6) A peculiar result from the set of 12 repeated measurements of the PPD of the electrostatic tube at 12 kV (Fig. 6b) is the 129% statistical counting efficiency value. Such an impossibly high figure, of course, cannot be correct. Another set of repeated measurements were made to clarify the first set, but the later experiment failed to convincingly confirm, or deny, the first result. Once again, the low-power statistical values were very noisy. However, the agreement of the statistical values in the region of the valley between the two peaks was very good, and gives a value of 100% at that point. We believe this value is the correct one. Certainly, the peculiar result of greater than 100% counting efficiency at 0 pulse power is unrepresentative of other tests of the electrostatic P-47 tube, and of all other tubes.

VI. X-3 PHOSPHORS

We very recently have made measurements of two Proxitronic intensifiers having X-3 phosphor screens. The results are very similar for both tubes. The phosphor layer thickness in both tubes was optimized for dc gain based on tests of earlier tube samples, and the electron scrubbing dosage was chosen to be the same as has been found optimum for P-20s. Figure 3 shows the dc gain vs. voltage of one of the tubes and Fig. 8 gives the PPD and counting efficiency. It may be seen that the statistical counting efficiency for the X-3 phosphor is very similar to that of the P-47 phosphor, and again reaches the virtually ideal 100%. Thus, just as is the case for the P-47 phosphor, even though the sandwich gain of the X-3 phosphor is significantly lower than that of the P-20 phosphor, the PPD and counting efficiency are in fact superior.

VII. OTHER RELATED INTENSIFIER DEVELOPMENTS

Considerable intensifier development at Steward Observatory, funded through other sources, is of relevance to the overall NOSC program. We summarize some of the more related developments in this section.

1. Remarkable success has been achieved by Proxitronic in developing a green-peaked photocathode response to spectrally match the green output P-20 and X-3 phosphors, for use in gain-stage tubes. The latest three gain-stage tubes have had photocathode quantum efficiencies exceeding 12% at 5600 A, equalling the very best we have ever measured.

2. Of the 7 developmental Proxitronic gain stages examined, 1 is fully suitable as a final (eg, 4th) stage intensifier, 1 is suitable as an intermediate (eg, 3rd) stage, and 1 meets the stringent requirements as a 2nd staqe (no field emission, low dark emission, good photocathode response, good uniformity of response and good phosphor gain). With these tubes in hand, design and construction of our first multi-stage Proxitronic intensifier package is well underway. It is to be used in two modes at the MMT: as a photon-counting speckle camera, and as an analog rapid-guided high-resolution camera.

3. Proxitronic has continued to produce first-stage tubes that contain consistently excellent bialkali photocathodes (blue light quantum efficiencies exceeding 20%) in 1.5mm separation tube structures (the spacing required for sufficient resolution with a bialkali photocathode). Unfortunately, only one of the 3 tubes delivered during this study may be operated at adequate high voltage (10-12kV) before field emission sets in. Attempts by Steward Observatory and Proxitronic to surgically remove the

field emitting spots with various lasers were not generally successful, although Proxitronic did manage to remove one weak spot in the one satisfactory tube that now is free of field emission. We have concluded that the future manufacture of 1.5mm-separation, bialkali-photocathode tubes operable to 12 kV is simply not cost-effective, and that we must accept the lower-resolution 2.5mm separation tube configuration (cf. Cromwell et. al., 1985).

4. Early attempts at producing better blue-peaked multialkali photocathodes have been only moderately successful. Two early samples each had quantum efficiencies over the spectral range 3000-5500 A of 16-10%. Two first stage tubes with a blue-peaked multialkali photocathode just recently recieved (the X-3 phosphor tubes) have much better photocathodes, having quantum effieiencies of 22-10 % over the spectral range 3000-5500 A.

VIII. CONCLUSIONS

Several important results have been obtained regarding the dc gain, the single photoelectron counting efficiency and the PPD of P-20, P-47 and X-3 phosphors. The dc gain in Proxitronic P-20 intensifiers has been improved to a consistently very high figure (greater than 450 photons/15-kV-photoelectron) through optimizing the phosphor layer thickness and the electron scrubbing dosage. Similar optimizing has been carried out in Proxitronic X-3 phosphors, resulting in a gain figure of about 110 photons/15-kV-photoelectron. While no optimization process was undertaken for the ITT P-47 phosphors in the present study, the high counting efficiency of this phosphor at least demonstrates that the layer thickness is sufficient to prevent significant voids in the screen. The gains of the two P-47 tubes were measured to be 92 and 115 photons/15-kV-photoelectron, respectively. Sandwich gains with an appropriately matched photocathode fiberoptically coupled to these phosphors are characteristically around 60 for the P-20, 12 for the X-3 and 15 for the P-47. Higher figures could be expected for glass-out/glass-in coupling, such as used in the non-imaging NOSC hybrid detector.

Early samples of Proxitronic P-20 intensifiers were found to have insufficient phosphor screen thickness, resulting in about a 10% area of voids and a comensurate loss in gain and counting efficiency. However, of all the other screen production processes originally examined as candidates for causing lost counting efficiency, none was found to have an effect. To this date, we have been unable to duplicate the high counting efficiency (85%) exhibited by at least some Varo P-20 intensifier diodes manufactured in the late 70s and early 80s, nor have we determined why these phosphor screens were so good. The present optimized Proxitronic tubes exhibit as high a counting efficiency (60%) as any other P-20 (and P-11 and Z-151B) phosphor tubes we have examined in 15 years, with the exception of at least a few Varo tubes with the magic potion P-20.

The two ITT P-47 phosphor tubes and two Proxitronic X-3 phosphor tubes all exhibit virtually ideal 100% counting efficiencies when operated at 15 kV. This is in spite of the fact that neither phosphor has as high an energy efficiency as the P-20 in converting electrons to light (in both the dc gain measurements and the pulse power measurements).

At operating voltages of 10 kV and higher, all three phosphor types (P-20, P-47 and X-3) produce a double-peaked PPD. Although we had been uncertain of the second, low-power peak in earlier studies, the present two-dimensional photon counter is free enough of low-power noise to clearly discern its presence. The majority of pulses in the low-power peak represent a multiple-counting of the original photoelectron, and are thought

to possibly be caused by X-rays. This multiple counting gives rise to integrated raw counting efficiency values of greater than 100% at sufficiently low pulse powers. However, the statistical fluctuations in the pulses demonstrate that the true counting efficiency is substantially lower than the integrated raw counting efficiency at 0 power.

For the P-47 phosphor tubes, some initial tests were carried out at reduced operating voltages, tests of particular relevance to the NOSC application. As the voltage is lowered below about 10 kV, the division between the main peak and the low-power peak of the PPD becomes more and more obscure, and the main peak melds with the low-power peak. For pulse counting, this makes it increasingly difficult to discriminate between a true photoelectron pulse and a false multiple-counting event or other noise pulse at low powers. For analog detectors, such as the NOSC detector, the broadened PPD will degrade the noise factor of the system. At a voltage of 6 kV, the PPD is very skew toward low power, and some of the photoelectrons appear to become truly lost (73 % statistical counting efficiency).

Finally, from the extensive SEM tests of P-20 screens and from a comparison of multiple samples of operating P-20 tubes, we are forced to conclude that the lost photoelectron pulses in most P-20 screens is caused by a flaw that occurs during the initial manufacture of the P-20 powder. Our current hypothesis is that there exists insufficient activator density, and thereby insufficient target areas, in the presently manufactured P-20 powders. This is presumed to be true for other P-20, P-11 and Z-151B phosphors in tubes from various manufacturers that have exhibited low counting efficiencies (roughly 50%) as well. The high counting efficiency P-47 and X-3 phosphors are fabricated with activator densities typically 3 to 5 times that of P-20 powders. There is some evidence in our earlier work, where the counting efficiency of a P-20 phosphor remained fixed over a voltage range of 10-20 kV (Cromwell et. al., 1985), that there exists a high energy electron trapping mechanism in these phosphors that removes some of the electrons from hitting a target at all.

IX. RECOMMENDED FUTURE WORK

The present study has revealed solid evidence of a multiple counting and noise source in the low-power region of the PPD of the P-47 phosphor used in the NOSC detector (and other phosphors as well). The noise in this region has made it difficult to measure with confidence the shape of the true PPD of the true single photoelectrons in the low-power portion of the distribution, and the statistical counting efficiency is somewhat uncertain in this region as well, especially at the lower operating voltages. The two-dimensinal photon counter should allow us, with little additional development, to accurately assess the true counting efficiency in this region, and to determine what processes are involved in the multiple counting phenomenon. We recommend that this work be carried out using the present two ITT P-47 tubes. Of particular interest to the NOSC application is a careful determination of what the low threshold is of the diode operating voltage that results in photoelectron pulses being lost completely. Additional testing can determine this.

At best, at voltages greater than 10 kV, the PPD of the P-47 is very broad. It becomes even broader at reduced voltages, impairing the counting efficiency of pulse counters and impairing the noise factor of analog detectors. We highly recommend investigating the PPD and counting efficiency of other phosphors that may hold hope for improvement. One such class of phosphors appears to be thulium activated phosphors (with relatively high activator densities). There may be others that should be investigated.

We recommend constructing an intensifier having a P-20 phosphor with increased activator density, to investigate if the counting efficiency and/or PPD are improved.

Finally, we recommend carrying out an experiment using the NOSC analog readout system to measure the S/N vs. voltage (of front-end diode) under signal and background levels relevant to the NOSC task. A P-47 diode capable of operation up to 15 kV should be used in this experiment. The present PPD results show a voltage of 15 kV will likely provide a substantially more sensitive detector than one where the diode is operated at only 5-6 kV, as is currently being done with the NOSC detector.

REFERENCES

Allen, R.G., Cromwell, R.H., Liebert, J.W., Macklin, R.H., and Stockman, H.S. 1984, "The Steward Observatory Intensified Photon-Counting Reticon System," Instrumentation in Astronomy V, A. Boksenburg, D.L. Crawford, eds., Proceedings of the SPIE, 445, 168.

Cromwell, R.H., Strittmatter, P.A., Allen, R.G., Hege, E.K., Kuhr, H., Marien, K.-H., Funk, H.W., and Frank, K. 1985, "A Proximity Focused Image Intensifier for Astronomy," in Advances in Electronics and Electron Physics, Vol.64A, pp.77-92, B.L. Morgan and P.W. Hawkes, eds.

Cromwell, R.H. 1986, "Toward Solving the Lost Photon Problem in Image Intensifiers," Instrumentation in Astronomy VI, D.L. Crawford, ed., Proceedings of the SPIE, 627, 610.

Hege, E.K., Cromwell, R.H. and Woolf, N.J. 1979, "Quantum-Noise Limited Readout of Image Intensifiers Using a Reticon Photodiode Array," in Advances in Electronics and Electron Physics, Vol. 52, pp. 397-413, L. Marton and C. Marton, eds.

FIGURE CAPTIONS

Fig. 1. Schematic diagram of two-dimensional photon counter set up to measure the PPD and single photoelectron counting efficiency of a proximity focused diode intensifier tube.

Fig. 2. PPD of Big Red alone. Also shown at specific pulse powers are the cumulitive raw counting efficiency (R), the cumulitive statistical counting efficiency (S) and the standard deviation of the mean statistical counting efficiency. Relay lens set to f/1.4. Number of sets of 100-picture pairs: 3.

Fig. 3. DC gain vs. voltage for 4 different P-20 phosphors and one X-3 phosphor. The photons emitted by the phosphors are considered to be at a wavelength of 5600 A, near the peak spectral emission. The sandwich gain of a fiberoptically coupled phosphor/photocathode may be calculated by multiplying dc gain by the photocathode quantum efficiency at 5600 A. The phosphors shown are a representative Varo P-20, a recent optimized Proxitronic P-20 (A), an earlier improved Proxitronic P-20 (B), a standard Proxitronic P-20 (C) and a recent optimized Proxitronic X-3 (D).

Fig. 4. DC gain vs. voltage for the ITT electrostatic and proximity P-47 phosphor tubes. The two phosphors are virtually identical in intrinsic gain but differ in dead voltage (voltage intercept at 0 gain) presumably because of different aluminum layer thicknesses. The photons emitted by the phosphors are considered to be at a wavelength of 4250 A, near the peak spectral emission. The sandwich gain of a fiberoptically coupled phosphor/photocathode may be calculated by multiplying dc gain by the photocathode quantum efficiency at 4250 A. In a NOSC hybrid detector, the sandwich gain would be somewhat higher because of its glass/glass window coupling.

Fig. 5a. PPD, raw and statistical counting efficiencies of a Proxitronic P-20 phosphor operated at 12 kV. Although the cumulative raw counting efficiency at low powers exceeds 100 % due to multiple counting of single electrons in the low power second peak, the true counting efficiency, or cumulative statistical counting efficiency, plateaus to a value of roughly 56 %. Relay lens set to f/4 to examine the lower-power region of the PPD. Number of 100-picture pairs: 1.

Fig. 5b. PPD, raw and statistical counting efficiencies of the ITT electrostatic P-47 phosphor operated at 15 kV. As with the P-20 phosphor in Fig. 5a, the cumulative raw counting efficiency again exceeds 100 % due to multiple counting of single electrons in the low power peak, but the cumulative statistical counting efficiency plateaus to a value of virtually 100 % in this P-47 phosphor. Relay lens set to f/2.8 to examine the lower-power region of the PPD. Number of 100-picture pairs: 1.

Fig. 6a. PPD, raw and statistical counting efficiencies of the ITT electrostatic P-47 phosphor operated at 15 kV. Relay lens set to f/4, optimum for examining the entire range of pulse powers in a single experiment. Number of 100-picture pairs: 1. Figures 6a-c illustrate that the PPD becomes more and more skew toward lower power when the operating voltage is decreased, and suggest that some of the photoelectrons become truly lost at 6 kV (see text).

Fig. 6b. Same as Fig. 6a, only 12 kV. Relay lens set to f/3.3. Number of 50-picture pairs: 12.

Fig. 6c. Same as Fig 6a, only 8 kV. Relay lens set to f/2.8. Number of 100-picture pairs: 1.

Fig. 6d. Same as Fig 6a, only 6 kV. Relay lens set to f/2.8. Number of 100-picture pairs: 1.

Fig. 7a. PPD, raw and statistical counting efficiencies of the ITT proximity P-47 phosphor operated at 15 kV. Relay lens set to f/4. Number of 100-picture pairs: 3 in 7a, 2 in 7b, 1 in 7c. Pulses counted in Fig. 7a arise within the proximity-focused area of the original image. Pulses counted in Fig. 7b arise outside the area of the true image, and are caused by light transmitted and scattered within the tube structure. The true counting efficiency for this tube is the sum of the value shown in Fig. 7a plus the respective value in Fig. 7b. Therefore, the true counting efficiency is very near 100 %. Fig. 7c shows the PPD of single electrons from Big Red alone under test conditions identical to those of Figs. 7a and b. Only the brightest third of Big Red's PPD is captured under these conditions.

Fig. 7b. See caption to Fig. 7a.

Fig. 7c. See caption to Fig. 7a.

Fig. 8. PPD, raw and statistical counting efficiencies of a Proxitronic X-3 phosphor operated at 15 kV. The statistical counting efficiency for the X-3 phosphor is very similar to that of the P-47 phosphor, and again reaches the virtually ideal 100 %.

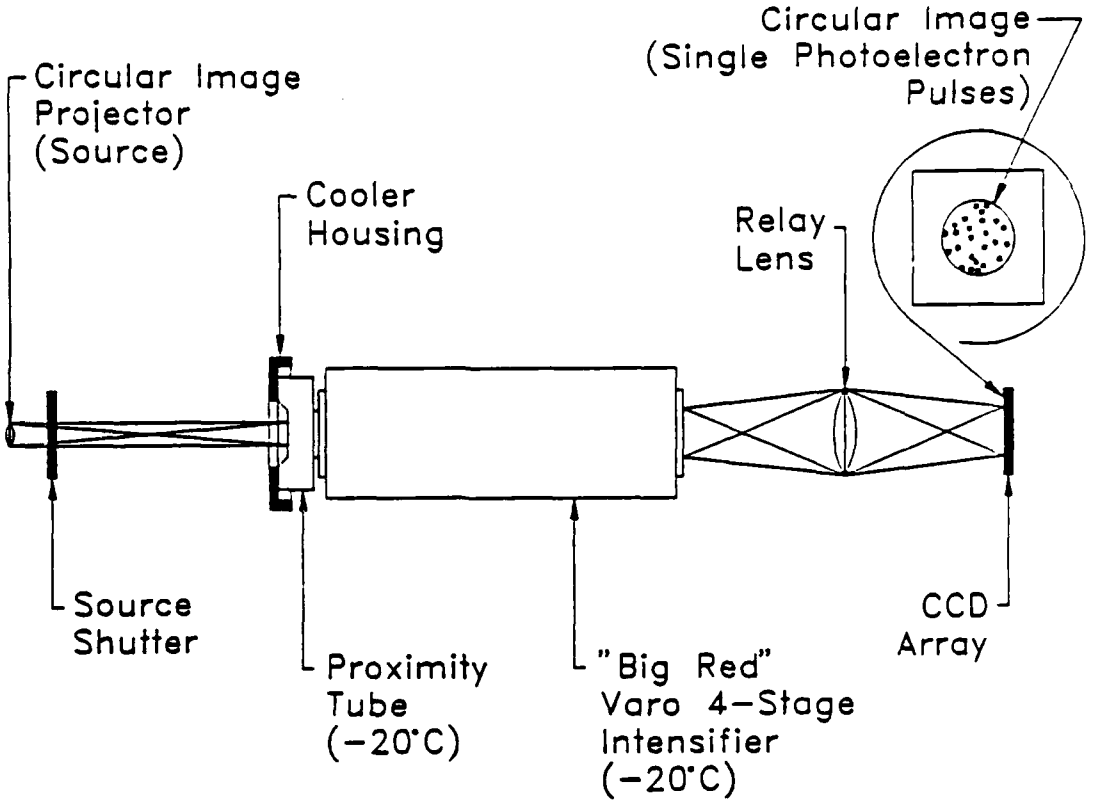

FIGURE 1

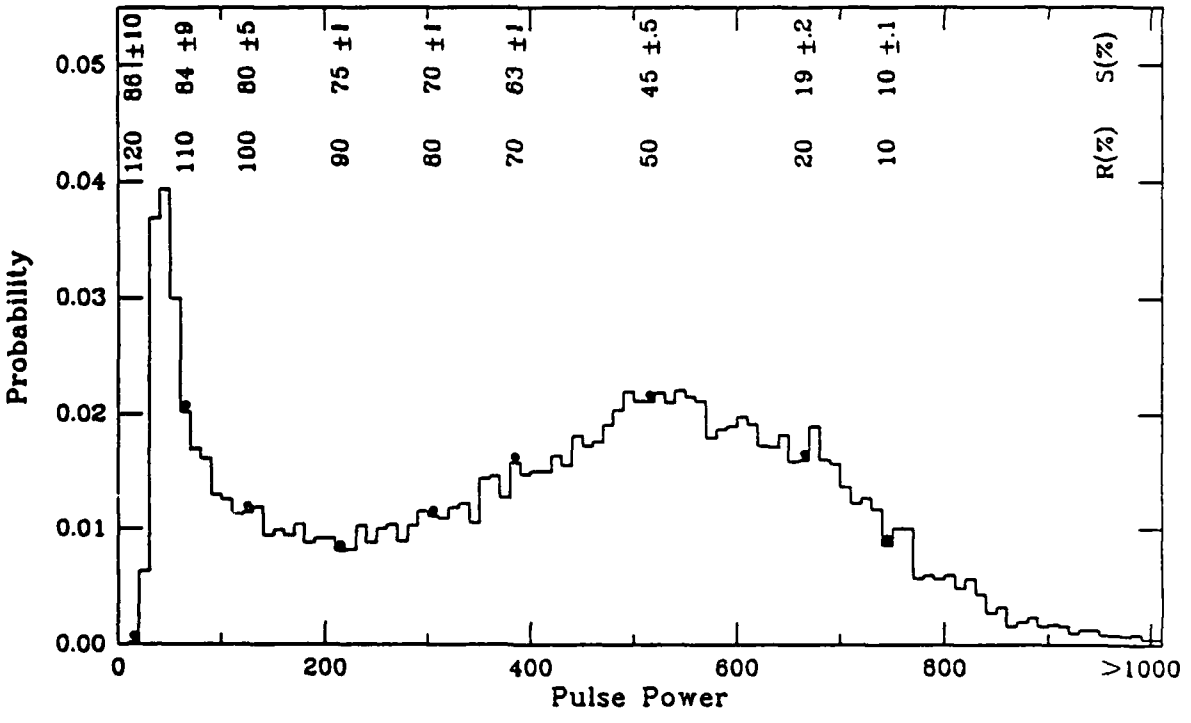

FIGURE 2

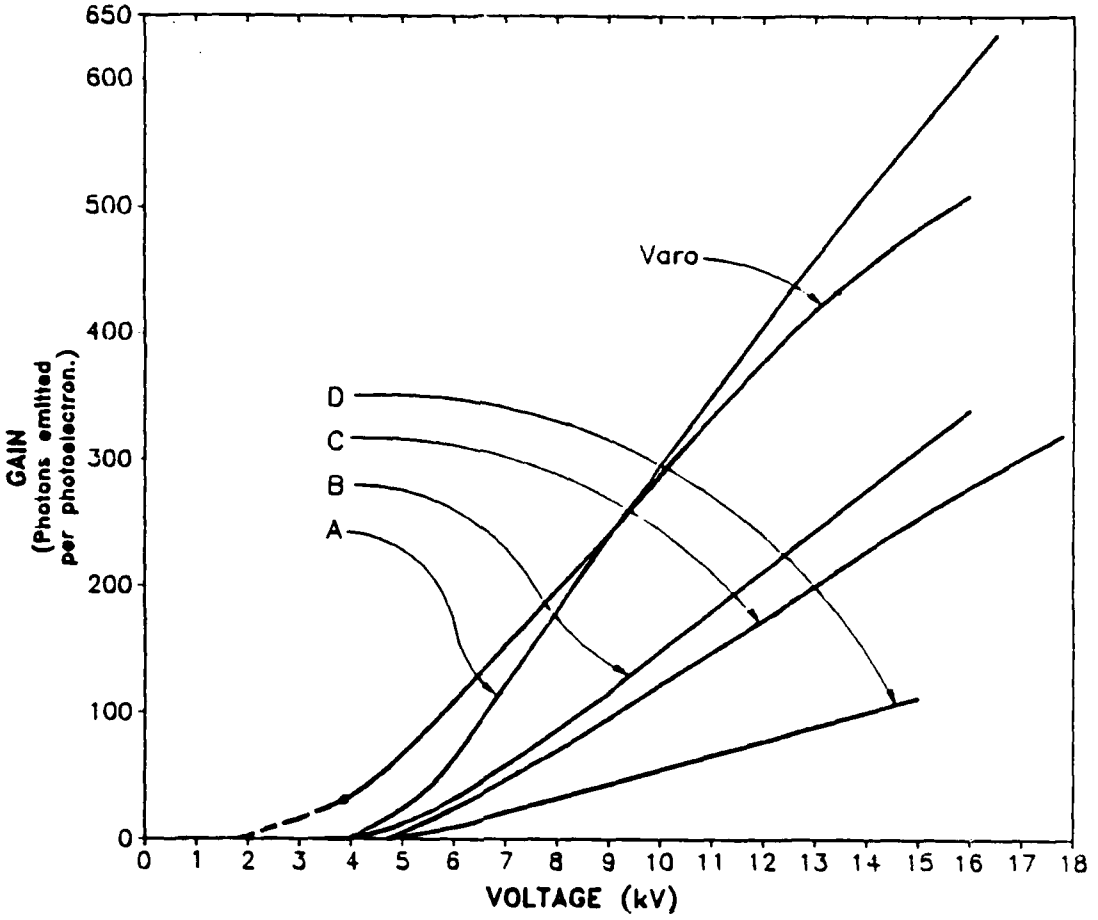

FIGURE 3

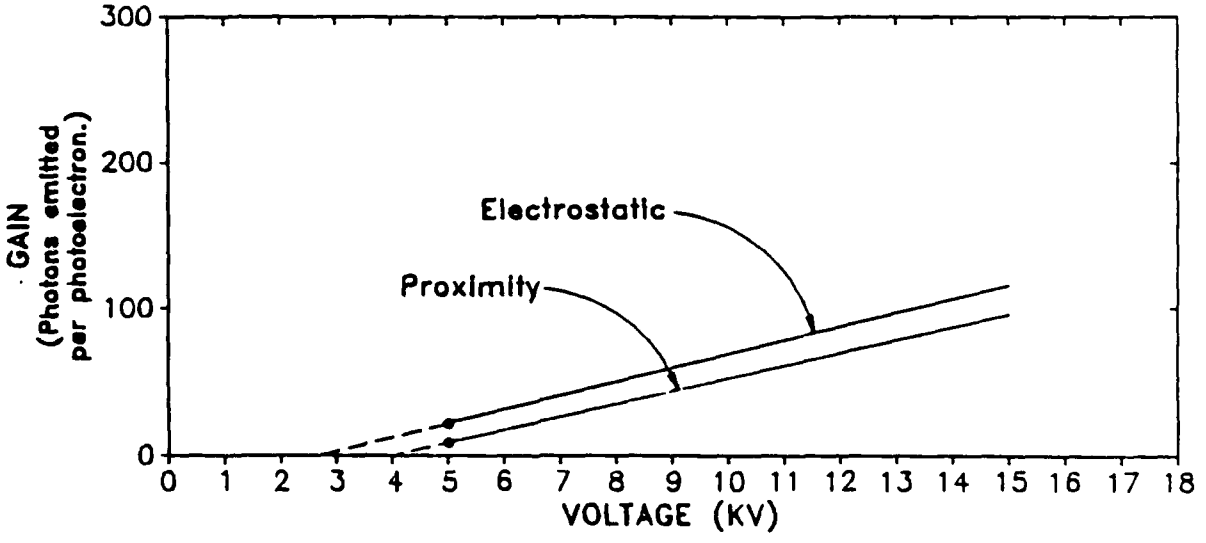

FIGURE 4

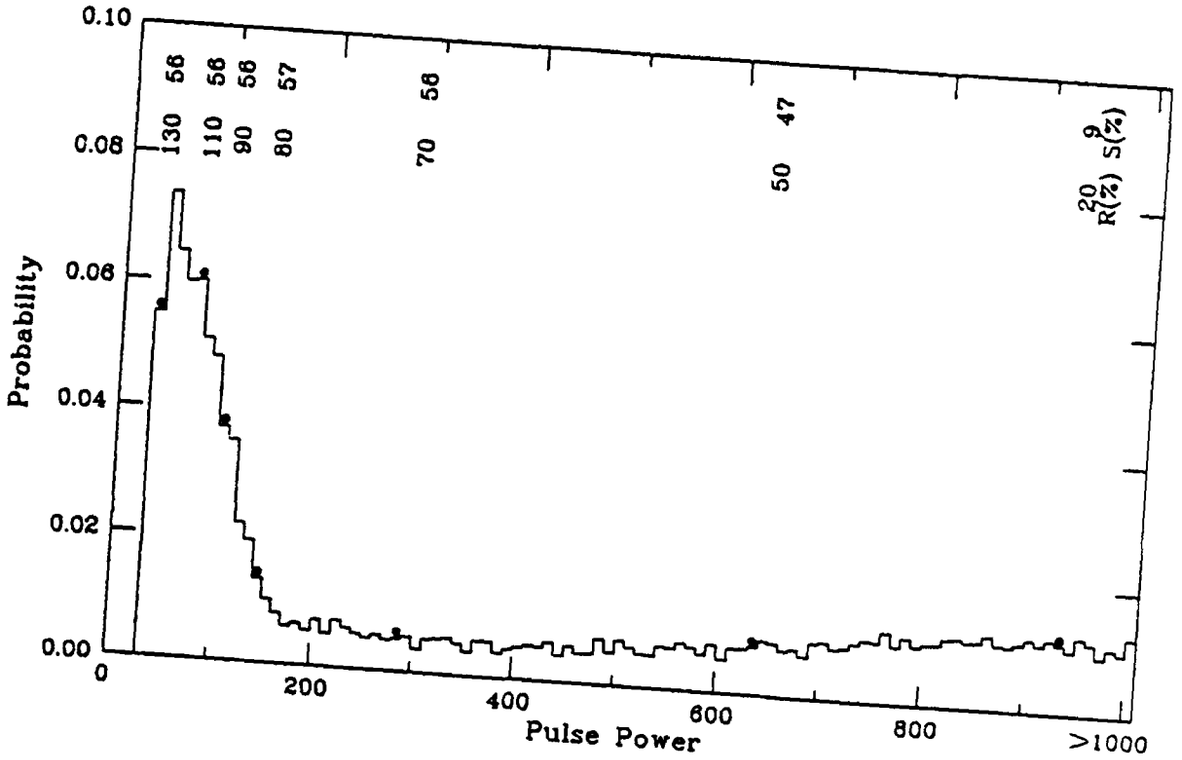

FIGURE 5a

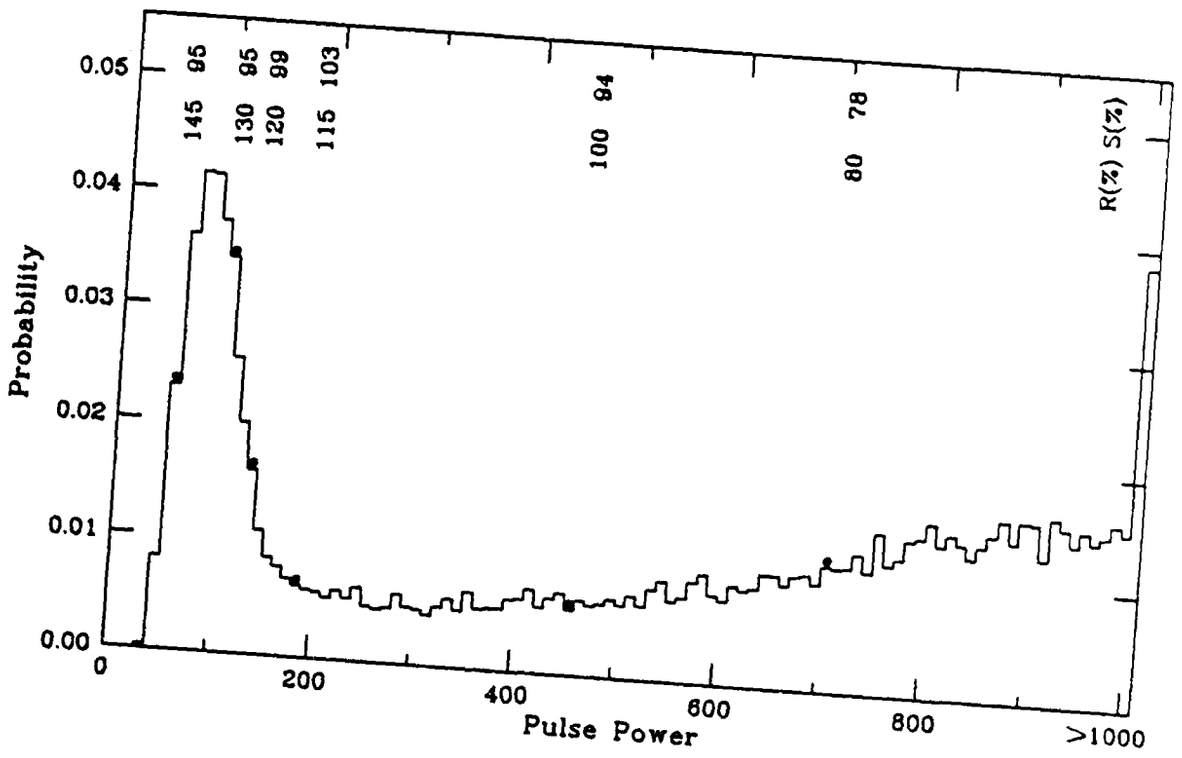

FIGURE 5b

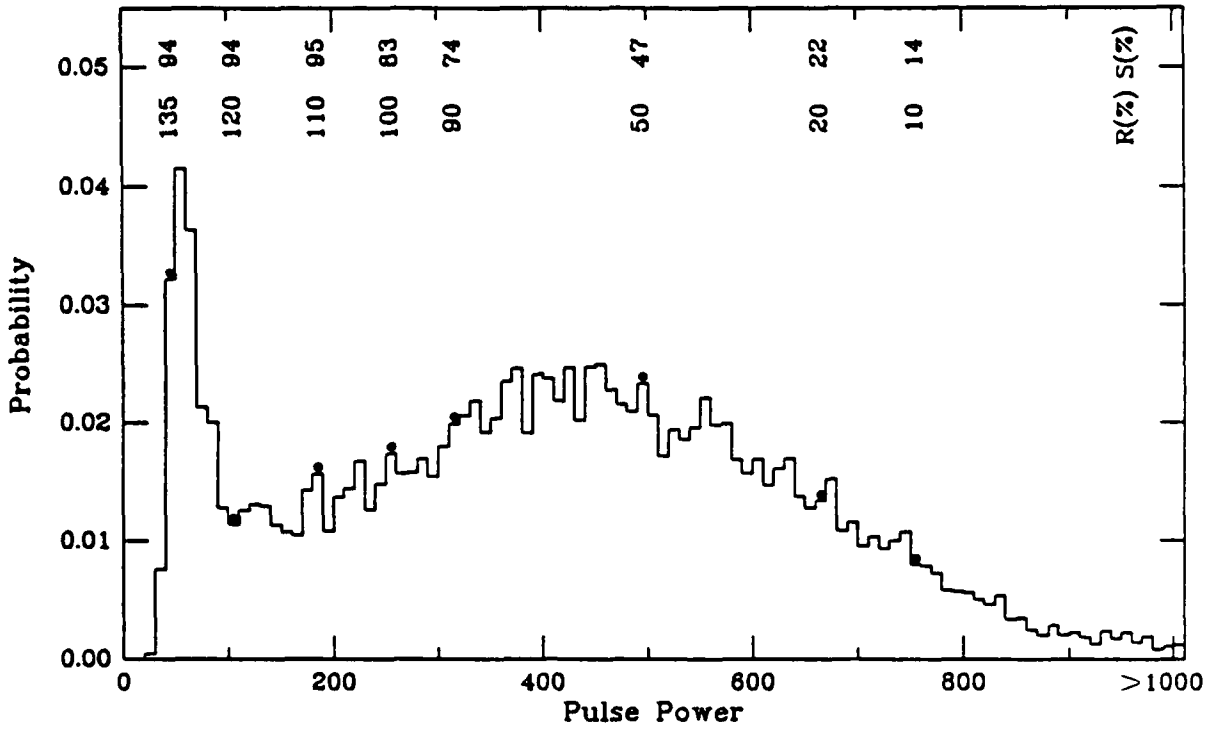

FIGURE 6a

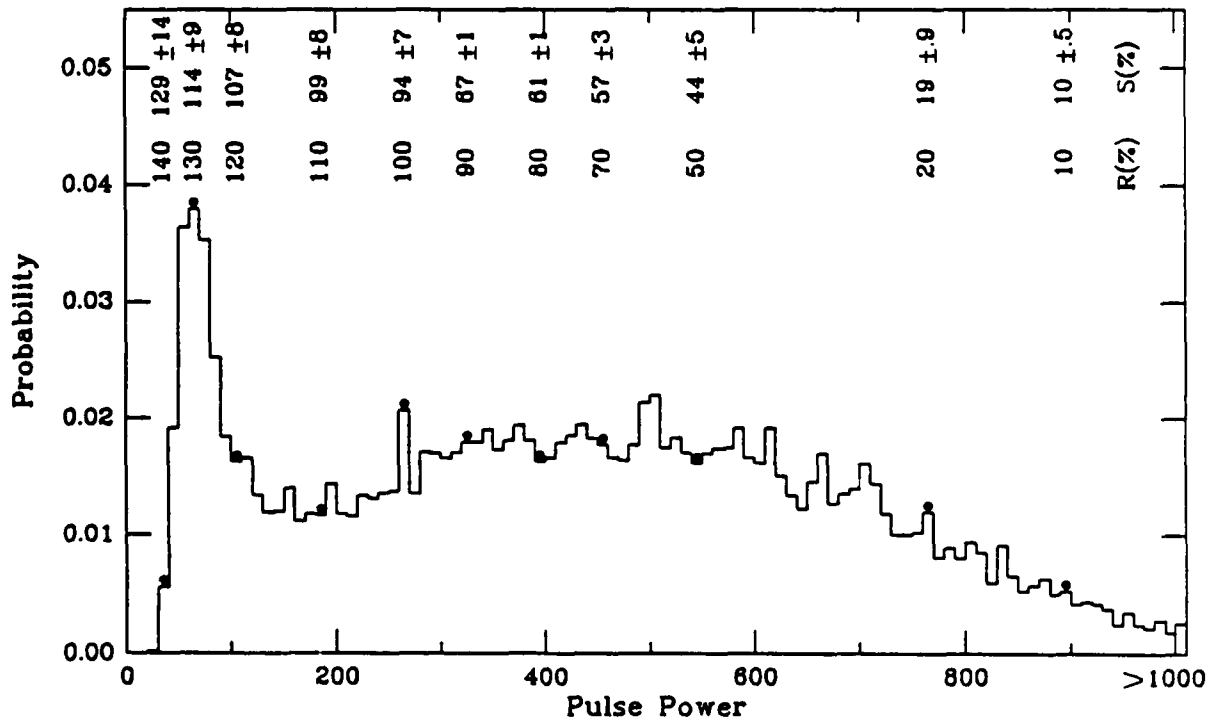

FIGURE 6b

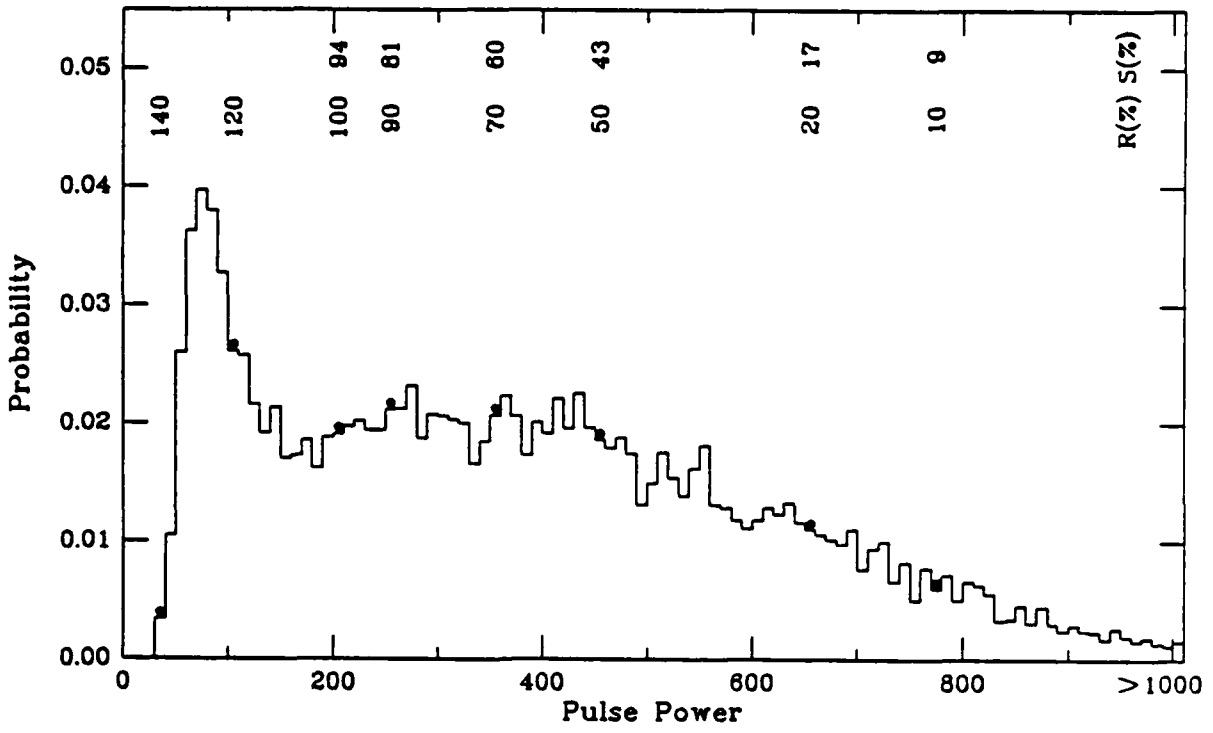

FIGURE 6c

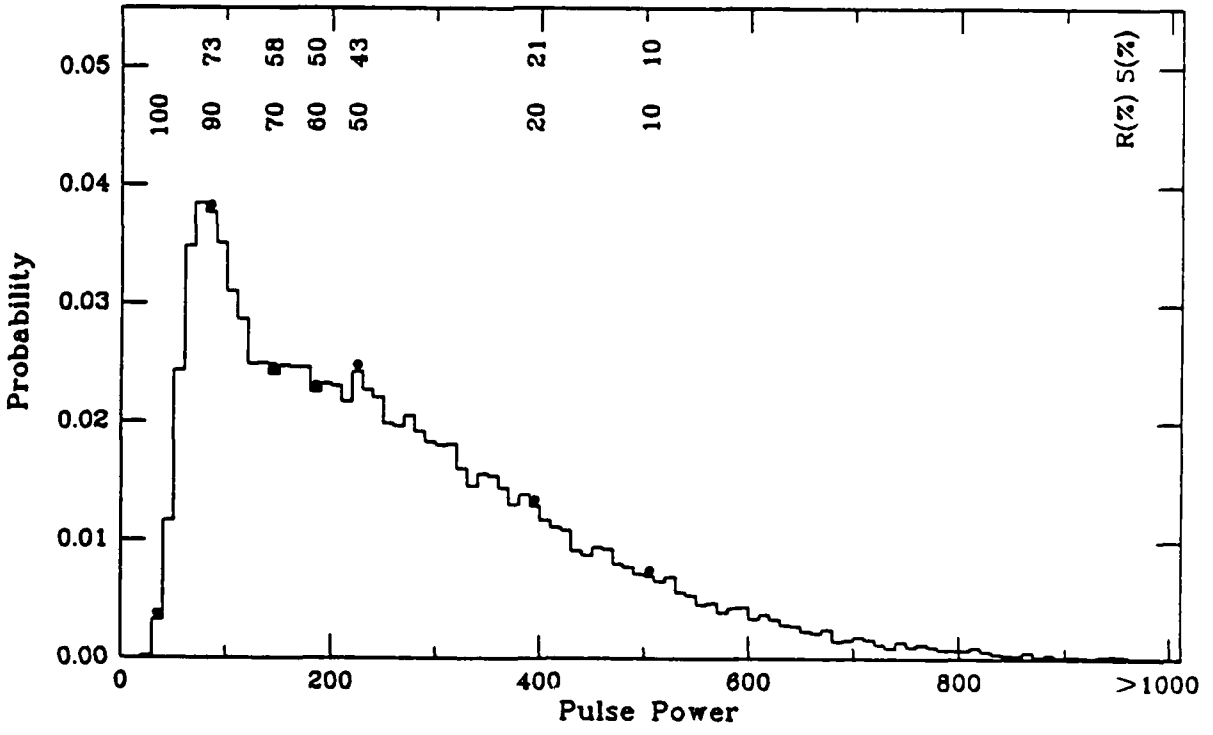

FIGURE 6d

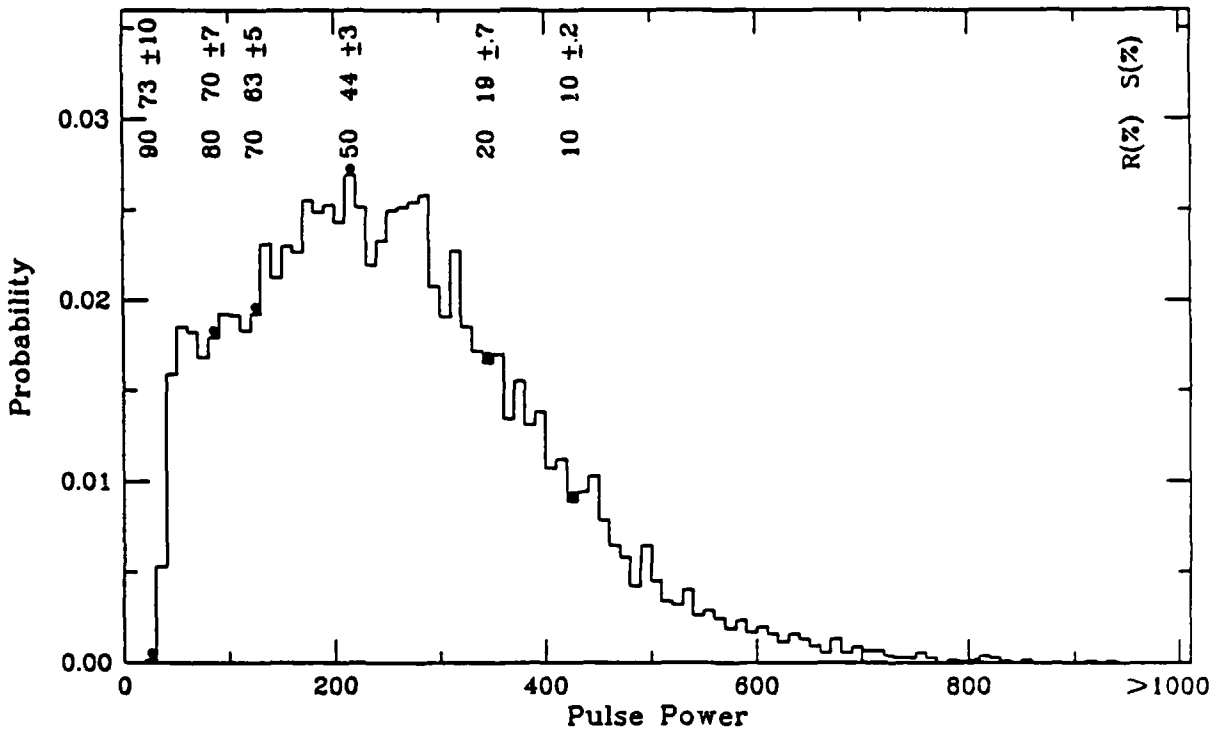

FIGURE 7a

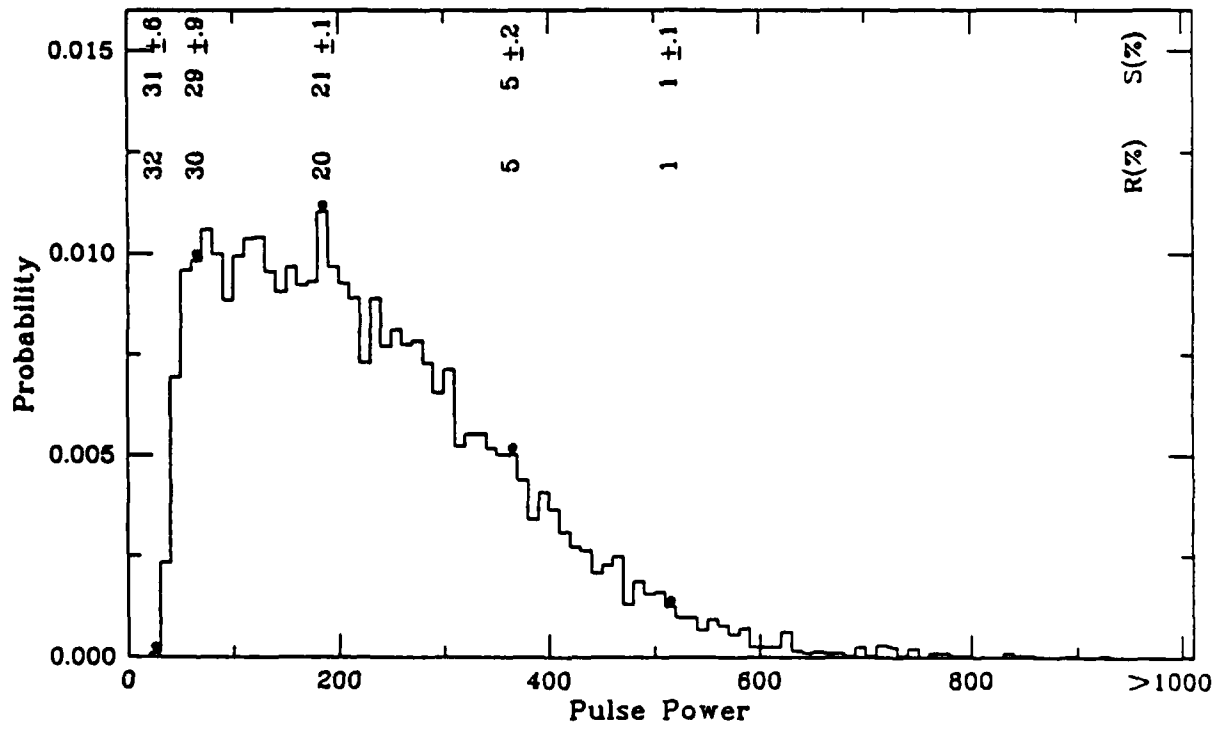

FIGURE 7b

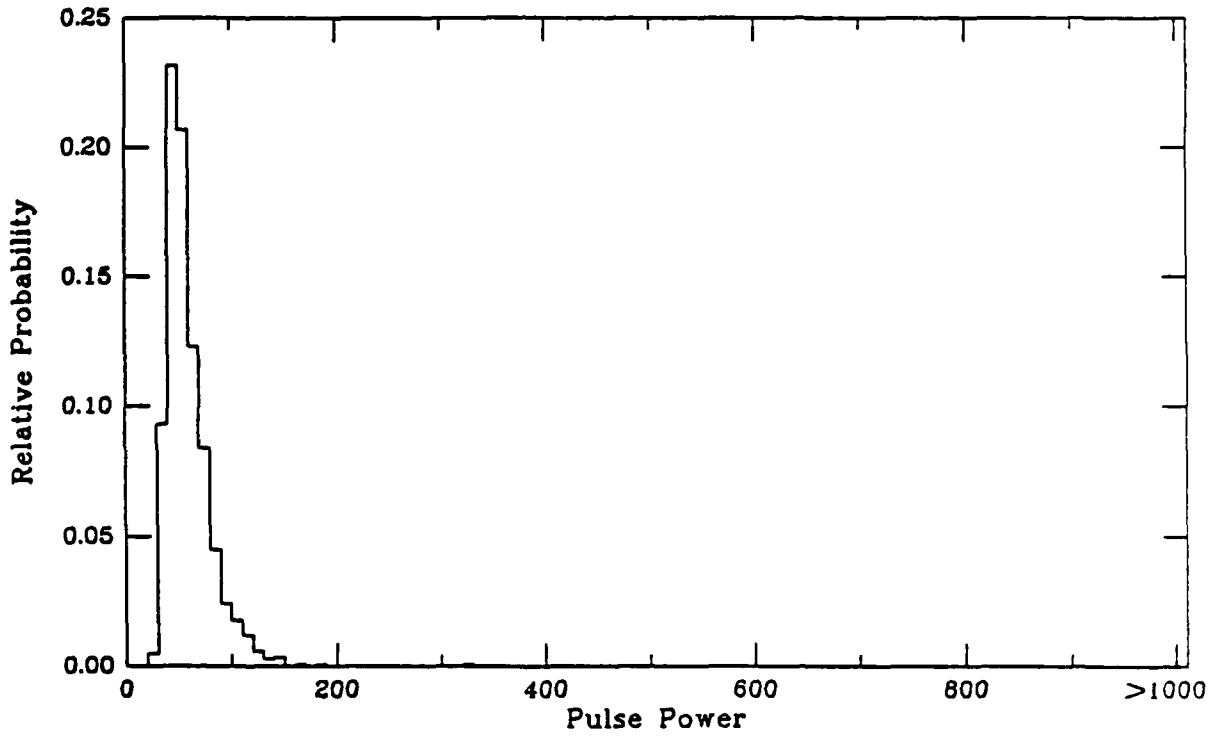
0.25
0.20
0.15
0.10
0.05
0.00
Relative Probability
0
200
400
600
800
>1000
Pulse Power

FIGURE 7c

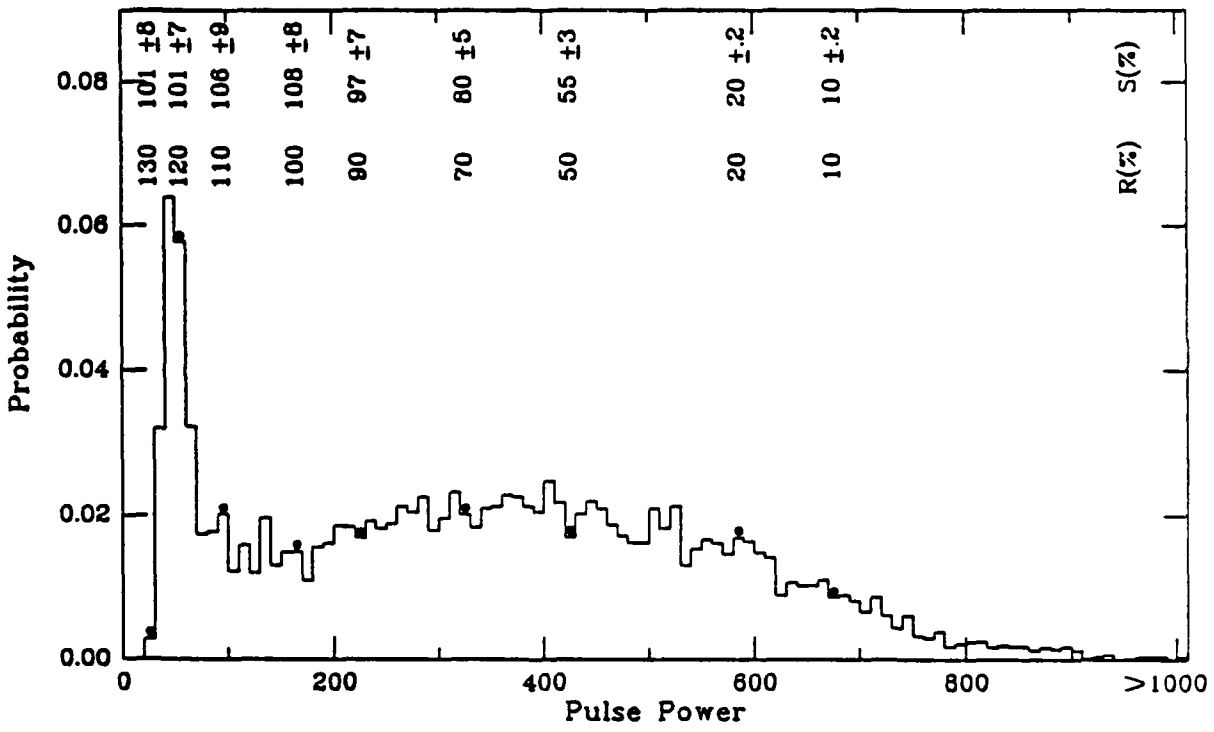
101 ±8
101 ±7
106 ±9
108 ±8
97 ±7
80 ±5
55 ±3
20 ±.2
10 ±.2
S(%)
130
120
110
100
90
70
50
20
10
R(%)
0.08
0.06
0.04
0.02
0.00
Probability
0
200
400
600
800
>1000
Pulse Power

FIGURE 8

REPORT DOCUMENTATION PAGE

Form Approved
OMB No. 0704-0188

1. AGENCY USE ONLY *(Leave blank)*	2. REPORT DATE	3. REPORT TYPE AND DATES COVERED
	April 1990	Final: Sep 1986 to Dec 1988

4. TITLE AND SUBTITLE

GAIN, PULSE POWER DISTRIBUTION, AND SINGLE ELECTRON COUNTING EFFICIENCY OF P-20, P-47, AND X-3 PHOSPHORS

5. FUNDING NUMBERS

C: N66001-86-C-0311
WU: DN307474

6. AUTHOR(S)

7. PERFORMING ORGANIZATION NAME(S) AND ADDRESS(ES)

Steward Observatory
University of Arizona
Tucson, AZ 85721

8. PERFORMING ORGANIZATION REPORT NUMBER

9. SPONSORING/MONITORING AGENCY NAME(S) AND ADDRESS(ES)

Naval Ocean Systems Center
San Diego, CA 92152-5000

10. SPONSORING/MONITORING AGENCY REPORT NUMBER

NOSC TD 1799

11. SUPPLEMENTARY NOTES

12a. DISTRIBUTION/AVAILABILITY STATEMENT

Approved for public release; distribution is unlimited.

12b. DISTRIBUTION CODE

13. ABSTRACT *(Maximum 200 words)*

This document summarizes analysis made of the dc gain, pulse power distribution (PPD), and single photoelectron counting efficiency of P-20, P-47, and X-3 phosphors.

14. SUBJECT TERMS

pulse power distribution (PPD)
dc gain

15. NUMBER OF PAGES

34

16. PRICE CODE

17. SECURITY CLASSIFICATION OF REPORT	18. SECURITY CLASSIFICATION OF THIS PAGE	19. SECURITY CLASSIFICATION OF ABSTRACT	20. LIMITATION OF ABSTRACT
UNCLASSIFIED	UNCLASSIFIED	UNCLASSIFIED	SAME AS REPORT